E-ISSN 2586-9027
Homepage : https://tci-thaijo.org/index.php/SciTechAsia Science & Technology Asia
Vol.31 No.3 July - September 2026 Page: [76-91]
Original research article

The Marshall-Olkin Extended Circular Uniform (MOECU) Distribution: Its Properties and Application

Phani Yedlapalli[1], Ch. Shashi Kumar[2,*]

[1]*Department of Mathematics, Vishnu Women's University, Andhra Pradesh 534202, India*
[2]*Department of Mathematics, VNR Vignana Jyothi Institute of Engineering and Technology, Telangana 500118, India*

Received 9 July 2026; Received in revised form 1 September 2026
Accepted 7 September 2026; Available online 30 September 2026

ABSTRACT

Circular data arise naturally in numerous scientific fields, including meteorology, biology, geology, environmental sciences, and directional statistics. The development of flexible circular distributions capable of modeling asymmetric angular observations remains an active area of research. In this article, we introduce the Marshall-Olkin Extended Circular Uniform (MOECU) distribution, a new one-parameter circular distribution on the interval $[0, 2\pi)$, obtained by applying the Marshall-Olkin transformation to the circular uniform baseline distribution. The proposed model possesses a simple closed-form probability density function, cumulative distribution function, and quantile function. We derive the characteristic function and trigonometric moments, establish a reflection symmetry linking α and $1/\alpha$, and obtain the population characteristics, hazard rate, mode and median. The parameter is estimated by maximum likelihood, whose asymptotic variance and confidence interval are derived in closed form; finite-sample performance is investigated through simulation alongside a method-of-moments estimator and eight classical goodness-of-fit-based estimators. The distribution is applied to the classical starhead topminnow orientation data and compared with several competing circular models through standard goodness-of-fit measures. The results demonstrate that MOECU is an effective and parsimonious alternative for modeling asymmetric circular data with competitive performance in practical applications.

Keywords: Circular model; Circular data; Marshall-Olkin distribution; Population characteristics; Starhead Topminnows

***Corresponding author:** skch17@gmail.com doi.org/10.70730/sta.v31i3.266746

1. Introduction

Directional or circular data frequently arise in many scientific disciplines where observations are measured as angles on the unit circle, i.e., in the interval $[0, 2\pi)$, where $\pi \approx 3.14159$ denotes the usual ratio of a circle's circumference to its diameter. Examples include wind directions in meteorology, animal movement orientations in biology, geological fracture directions, ocean current directions, and time-of-day phenomena. Unlike linear data, circular observations possess a periodic structure in which $\theta = 0$ and $\theta = 2\pi$ represent the same point on the circle. Consequently, traditional statistical methods developed for linear data are often inappropriate for the analysis of directional observations, motivating the development of specialized circular probability distributions.

Over the past decades, a number of circular distributions has been derived in the literature. Among the most widely used are the von Mises, wrapped Cauchy, wrapped normal, and cardioid distributions. Although these distributions have proven useful in many practical situations, they are symmetric (or symmetric up to a location shift) and may therefore exhibit limitations when modeling asymmetric directional data or datasets displaying distributional features that depart from the assumptions of classical circular models. This has encouraged researchers to develop new families of circular distributions with enhanced flexibility and improved fitting capabilities. More recently, a substantial body of work has focused on wrapping and projecting flexible linear distributions onto the circle; examples include the wrapped exponential distribution [3], the wrapped Laplace distribution [4], wrapped logistic [5], the wrapped weighted exponential [6], the stereographic circular logistic distribution [7], wrapped Lindley distribution [8], the wrapped transmuted exponential [9], the wrapped Akash [10], the wrapped two parameter Lindley distribution [11], the wrapped quasi-Lindley distribution [12], the wrapped modified Lindley [13], the wrapped XLindley distribution [14], the wrapped length biased exponential distribution [15], the wrapped size biased gamma Lindley distribution [16], and the wrapped Epanechnikov distribution [17], among others.

A complementary and less explored technique for developing new circular distributions is to apply a general distribution-generating mechanism directly to a circular baseline distribution, rather than to a linear distribution that is subsequently wrapped or projected. One widely used mechanism of this type is the Marshall-Olkin (MO) family [1], originally proposed for linear random variables. For a baseline cumulative distribution function (cdf) F with survival function $\bar{F} = 1 - F$, the Marshall-Olkin generalized survival function is $\bar{G}(y;\alpha) = \alpha\bar{F}(y) \times \left[1 - (1-\alpha)\bar{F}(y)\right]^{-1}$, $\alpha > 0$, which introduces a single additional tilt parameter α while retaining the mathematical tractability of the parent distribution, and reduces to F itself when $\alpha = 1$. The Marshall-Olkin technique has been employed extensively to generalize linear distributions, but its application to circular baselines has received comparatively little attention.

Motivated by these considerations, in this article we apply the Marshall-Olkin transformation directly to the circular uniform distribution, whose cdf on $[0, 2\pi)$ is $F(\theta) = \theta \times (2\pi)^{-1}$. Because the tilt parameter α continuously reweights probability mass toward one endpoint of the support while preserving the closed-form tractability of the uniform baseline, the resulting Marshall-Olkin Circular Uniform

(MOECU) distribution is, by construction, capable of representing markedly asymmetric, boundary-concentrated angular data – precisely the kind of departure from symmetry that the classical circular models listed above cannot easily accommodate. Sections 2–4 quantify this flexibility through the density shape, the hazard rate, and the population characteristics, and Section 7 shows that it translates into a fit that is at least as good as, and in most respects better than, several more heavily parameterized competitors on real data. MOECU admits a simple analytical expression for its probability density function (pdf), cumulative distribution function (cdf), and quantile function; its closed-form quantile function facilitates straightforward random variate generation and simulation studies. The main contributions of this article are summarized as follows:

(i) A new circular distribution with simple analytical structure is introduced;

(ii) Several mathematical properties of the distribution are derived, including its distributional and shape characteristics, and a reflection symmetry relating α and $1/\alpha$;

(iii) Parameter estimation is developed using the method of maximum likelihood, together with its asymptotic variance and confidence interval, and a method-of-moments alternative;

(iv) The finite-sample performance of the estimators is investigated through Monte Carlo simulation experiments across a wide range of parameter values and sample sizes;

(v) The applicability of the proposed model is demonstrated through application to a real circular dataset on starhead topminnow orientations, with comparisons against existing competing distributions.

The remainder of the article is organized as follows. Section 2 introduces the proposed distribution and establishes its validity as a circular distribution. Section 3 derives its statistical properties. Section 4 presents its population characteristics and the reflection symmetry. Section 5 discusses parameter estimation. Section 6 presents the results of the simulation study. Section 7 illustrates the practical applicability of the distribution using real data. Finally, Section 8 concludes the article with a summary of the main findings and possible directions for future research.

2. MO-Circular Uniform Distribution

2.1 Synthesis of the proposed distribution

Let Θ_0 denote a circular uniform random variable on $[0, 2\pi)$, with cumulative distribution function and probability density function respectively,

$$F(\theta) = \frac{\theta}{2\pi}, \qquad f(\theta) = \frac{1}{2\pi}, \qquad (2.1)$$

for $0 \le \theta < 2\pi$.

Applying the Marshall-Olkin transformation to F gives the cumulative distribution function

$$G(\theta;\alpha) = \frac{\alpha F(\theta)}{1-(1-\alpha)F(\theta)} = \frac{\alpha\theta}{2\pi-(1-\alpha)\theta}, \qquad (2.2)$$

for $0 \le \theta < 2\pi$ and $\alpha > 0$.

Theorem 2.1. *For every $\alpha > 0$, $G(\theta;\alpha)$ in Eq. (2.2) is a valid circular cumulative distribution function on $[0, 2\pi)$.*

Proof. (i) *Boundary conditions.* $G(0;\alpha) = 0$, and

$$\lim_{\theta\to 2\pi^-} G(\theta;\alpha) = \frac{2\pi\alpha}{2\pi-(1-\alpha)2\pi} = \frac{2\pi\alpha}{2\pi\alpha} = 1.$$

(ii) *Positivity.* For $\theta \in [0, 2\pi)$ and $\alpha > 0$,

$$2\pi-(1-\alpha)\theta \ \ge\ 2\pi-(1-\alpha)2\pi = 2\pi\alpha > 0$$

when $0 < \alpha \leq 1$, and the denominator is increasing in θ when $\alpha > 1$. Thus $G(\theta;\alpha)$ is well defined and finite on the support.

(iii) *Monotonicity.* Differentiating Eq. (2.2),

$$\begin{aligned} g(\theta;\alpha) &= \frac{d}{d\theta}G(\theta;\alpha) \\ &= \frac{\alpha\big(2\pi-(1-\alpha)\theta\big)+\alpha(1-\alpha)\theta}{\big(2\pi-(1-\alpha)\theta\big)^2} \\ &= \frac{2\pi\alpha}{\big(2\pi-(1-\alpha)\theta\big)^2} > 0, \end{aligned}$$

for all $\theta \in [0, 2\pi)$ and $\alpha > 0$, so G is strictly increasing. Since $g(\theta;\alpha) \geq 0$ on the support and $\int_0^{2\pi} g(\theta;\alpha)\, d\theta = 1$, g is a genuine probability density function and G is a valid circular cumulative function. □

Remark 2.2 (Identifiability)**.** *Differentiating (2) with respect to α gives $\partial G(\theta;\alpha)/\partial\alpha = \theta(2\pi-\theta)/\big(2\pi-(1-\alpha)\theta\big)^2 > 0$ for every $\theta \in (0, 2\pi)$, so $\alpha \mapsto G(\cdot;\alpha)$ is strictly increasing (in the pointwise order) and hence injective: distinct values of α produce distinct distributions. This identifiability property is used in Section 5.1.*

2.2 Probability density function

From the proof above, the density function of the Marshall-Olkin Extended Circular Uniform (MOECU) distribution is

$$\begin{aligned} g(\theta;\alpha) &= \frac{2\pi\alpha}{\big(2\pi-(1-\alpha)\theta\big)^2} \\ &= \frac{\alpha}{2\pi}\left[1-(1-\alpha)\frac{\theta}{2\pi}\right]^{-2}, \quad (2.3) \end{aligned}$$

for $0 \leq \theta < 2\pi$, $\alpha > 0$.

Remark 2.3. *Eq. (2.3) has the general Marshall-Olkin density form*

$$g(\theta;\alpha) = \frac{\alpha f(\theta)}{\big[1-(1-\alpha)F(\theta)\big]^2},$$

confirming that MOECU is precisely the MO-generalized circular uniform.

2.3 Shape behavior

From Eq. (2.3), $g(\theta;\alpha)$ is monotone in θ for every fixed α. Differentiating,

$$g'(\theta;\alpha) = \frac{4\pi\alpha(1-\alpha)}{\big(2\pi-(1-\alpha)\theta\big)^3},$$

whose sign, for $\theta \in [0, 2\pi)$, is the sign of $(1-\alpha)$ (the denominator is positive throughout the support by part (ii) of Theorem 1). Hence $g(\theta;\alpha)$ is *strictly increasing* on $[0, 2\pi)$ when $0 < \alpha < 1$, constant when $\alpha = 1$ (uniform), and *strictly decreasing* when $\alpha > 1$; there is no interior stationary point for $\alpha \neq 1$. Consequently the density is unimodal in the boundary sense, with its mode located at $\theta \to 2\pi^-$ for $\alpha < 1$ (mass concentrated near the reference direction from the "other side") and at $\theta = 0$ for $\alpha > 1$ (mass concentrated at the reference direction itself). This is confirmed directly by numerical maximization of Eq. (2.3) and is consistent with the median formula Eq. (3.2) below, since $\theta_{\text{median}}(\alpha) \to 2\pi$ as $\alpha \to 0^+$ and $\theta_{\text{median}}(\alpha) \to 0$ as $\alpha \to \infty$. This boundary-concentrated, monotone density behavior is well suited to angular data that cluster near a fixed reference direction with a long, decaying tail around the circle, as illustrated in Fig. 1.

3. Statistical Properties

3.1 Quantile function

Solving $G(\theta;\alpha) = u$ for θ in Eq. (2.2) gives the closed-form quantile function

$$Q(u,\alpha) = \frac{2\pi u}{\alpha+(1-\alpha)u}, \qquad (3.1)$$

for $0 \leq u < 1$, which permits direct random variate generation via $\Theta = Q(U;\alpha)$ for $U \sim \text{Uniform}(0, 1)$, with no need for rejection sampling or numerical inversion.

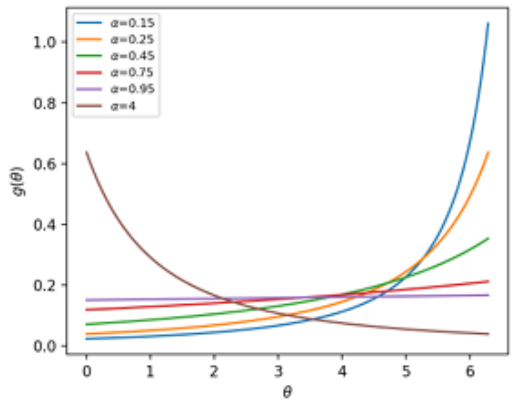


Fig. 1. MOECU density for several values of the parameter α; the density increases in θ for $\alpha < 1$ and decreases in θ for $\alpha > 1$.

3.2 Median

The circular median is obtained from Eq. (3.1) at $u = 0.5$,

$$\theta_{\text{median}}(\alpha) = \frac{2\pi}{1+\alpha}. \tag{3.2}$$

As $\alpha \to 0^+$, $\theta_{\text{median}} \to 2\pi$; as $\alpha \to \infty$, $\theta_{\text{median}} \to 0$, and $\theta_{\text{median}}(1) = \pi$, as expected for the uniform baseline, and consistent with the shape behavior established in Section 2.3.

3.3 Hazard rate

The circular hazard rate is

$$\delta(\theta;\alpha) = \frac{g(\theta;\alpha)}{1-G(\theta;\alpha)} = \frac{2\pi\alpha}{\big(2\pi-(1-\alpha)\theta\big)(2\pi-\theta)}. \tag{3.3}$$

For $\alpha = 1$, $\delta(\theta;1) = \dfrac{1}{2\pi-\theta}$, the increasing hazard rate of the uniform baseline. For general α, write $b = 1-\alpha$ and $D(\theta) = \big(2\pi - b\theta\big)(2\pi-\theta)$, so that $\delta(\theta;\alpha) = 2\pi\alpha/D(\theta)$ and δ is increasing exactly where D is decreasing. Since $D'(\theta) = -2\pi(1+b)+2b\theta$ is affine in θ, $D'(0) = -2\pi(1+b), D'(2\pi) = 2\pi(b-1) = -2\pi\alpha < 0$ always. When $0 < \alpha \le 2$ (i.e., $b \ge -1$), $D'(0) \le 0$ as well, and since D' is affine with both endpoint values ≤ 0, $D'(\theta) < 0$ throughout $[0, 2\pi)$; hence $\delta(\theta;\alpha)$ is *monotone increasing* on the whole support, with $\delta(\theta;\alpha) \to \infty$ as $\theta \to 2\pi^-$ (as it must, since $G(\theta;\alpha) \to 1$ there). When $\alpha > 2$ (i.e., $b < -1$), $D'(0) > 0$ while $D'(2\pi) < 0$, so D' changes sign exactly once, at

$$\theta^* = \frac{\pi(1+b)}{b} = \frac{\pi(2-\alpha)}{1-\alpha} \in (0,\pi) \subset (0,2\pi),$$

so that δ *decreases* on $[0,\theta^*)$ and *increases* on $(\theta^*, 2\pi)$: for sufficiently large α the hazard rate is bathtub-shaped rather than monotone, although it still diverges as $\theta \to 2\pi^-$. This refines and corrects the earlier working assumption that the hazard rate simply mirrors the monotonicity of the density; the two coincide only for $0 < \alpha \le 2$.

3.4 Characteristic function and moments

The p^{th} trigonometric moment of a circular random variable Θ is $\varphi_p = E(e^{ip\Theta}) = \int_0^{2\pi} e^{ip\theta} g(\theta;\alpha)\, d\theta = \alpha_p + i\beta_p$, $p = 1, 2, 3, \ldots$, where $\alpha_p = E(\cos p\Theta)$ and $\beta_p = E(\sin p\Theta)$. Putting $a = \theta/(2\pi)$,

$b = 1-\alpha$, and integrating (3) by parts gives

$$\varphi_p(\alpha) = 1 - 2\pi i p\alpha \int_0^1 \frac{a\, e^{2\pi i p a}}{1-ab}\, da. \tag{3.4}$$

Integral Eq. (3.4) does not admit a closed form for $p \geq 1$ in general, so it is evaluated directly by numerical quadrature; an exception is $E(\Theta^2)$-type integrals without the oscillatory kernel, which do admit closed forms and are used in Section 5.1 below.

4. Population Characteristics

Using the first two trigonometric moments α_1, β_1 and α_2, β_2 from Section 3.4, the circular population characteristics [18] are:

$$\text{Mean direction: } \mu = \operatorname{atan2}(\beta_1, \alpha_1), \tag{4.1}$$

$$\text{Resultant length: } \rho_1 = \sqrt{\alpha_1^2 + \beta_1^2}, \tag{4.2}$$

$$\text{Circular variance: } V = 1 - \rho_1, \tag{4.3}$$

$$\text{Circular skewness: } \nu = \frac{\rho_2 \sin(\mu_2 - 2\mu)}{(1-\rho_1)^{3/2}}, \tag{4.4}$$

$$\text{Circular kurtosis: } \kappa = \frac{\rho_2 \cos(\mu_2 - 2\mu) - \rho_1^4}{(1-\rho_1)^2}, \tag{4.5}$$

where $\rho_2 = \sqrt{\alpha_2^2 + \beta_2^2}$ and $\mu_2 = \operatorname{atan2}(\beta_2, \alpha_2)$. Here $\operatorname{atan2}(y, z)$ denotes the two-argument arctangent, i.e., the argument (in $(-\pi, \pi]$) of the complex number $z + iy$; unlike the ordinary $\arctan(y/z)$, it uses the signs of both y and z to place the angle in the correct quadrant, which is essential here because α_1, β_1 (and α_2, β_2) can each be of either sign.

Proposition 4.1 (Reflection symmetry)**.** *For every $\alpha > 0$ and $\theta \in [0, 2\pi)$,*

$$g(\theta; 1/\alpha) = g(2\pi - \theta; \alpha).$$

Consequently $\rho_1(1/\alpha) = \rho_1(\alpha)$, $V(1/\alpha) = V(\alpha)$, $\kappa(1/\alpha) = \kappa(\alpha)$, while $\mu(1/\alpha) = -\mu(\alpha)$ and $\nu(1/\alpha) = -\nu(\alpha)$.

Proof. Direct substitution in Eq. (2.3) gives

$$g(2\pi - \theta; \alpha) = \frac{2\pi\alpha}{\big(2\pi\alpha + (1-\alpha)\theta\big)^2},$$

$$g(\theta; 1/\alpha) = \frac{2\pi/\alpha}{\big(2\pi - (1-1/\alpha)\theta\big)^2} = \frac{2\pi\alpha}{\big(2\pi\alpha + (1-\alpha)\theta\big)^2},$$

which are identical. Thus the density of $2\pi - \Theta$ under parameter α equals the density of Θ under parameter $1/\alpha$; the stated identities for ρ_1, V, κ (even functionals of the reflection) and for μ, ν (odd functionals) follow immediately from the standard relations $E[\cos p(2\pi - \Theta)] = E[\cos p\Theta]$ and $E[\sin p(2\pi - \Theta)] = -E[\sin p\Theta]$. □

Table 1 reports the population characteristics, calculated by numerical integration of Eq. (3.4) as described in Section 3.4, on a reciprocal-symmetric grid of α that makes Proposition 2 directly checkable: each pair $(\alpha, 1/\alpha)$ yields identical ρ_1, V, κ and mirror-image μ, ν.

The mean resultant length ρ_1 increases symmetrically as α moves away from 1 on the reciprocal scale (Table 1; Proposition 2), while the circular variance $V = 1 - \rho_1$ is maximized exactly at $\alpha = 1$. The sign of the mean direction and skewness reverses between $\alpha < 1$ and $\alpha > 1$, reflecting the reflection about $\theta = \pi$ established in Proposition 2 (and consistent with the mode locations discussed in Section 2.3).

5. Parameter Estimation

5.1 Maximum likelihood estimation and its asymptotics

Let $\theta_1, \theta_2, \ldots, \theta_n$ be a random sample from the MOECU(α) distribution.

Table 1. Population characteristics of the MOECU distribution, on a reciprocal-symmetric grid of α illustrating the reflection symmetry of Proposition 2.

α	μ (rad)	ρ_1	$V = 1 - \rho_1$	ν	κ
0.10	-0.6126	0.6461	0.3539	0.8598	2.1210
0.20	-0.8546	0.4817	0.5183	0.4836	0.7349
0.25	-0.9430	0.4216	0.5784	0.3864	0.4858
0.50	-1.2443	0.2182	0.7818	0.1494	0.0832
1.00	–	0.0000	1.0000	0.0000	0.0000
2.00	1.2443	0.2182	0.7818	-0.1494	0.0832
4.00	0.9430	0.4216	0.5784	-0.3864	0.4858
5.00	0.8546	0.4817	0.5183	-0.4836	0.7349
10.00	0.6126	0.6461	0.3539	-0.8598	2.1210

From Eq. (2.3), the log-likelihood function is

$$\ell(\alpha) = n\log(2\pi\alpha) - 2\sum_{i=1}^{n}\log\big(2\pi - (1-\alpha)\theta_i\big). \tag{5.1}$$

Differentiating with respect to α gives the score equation

$$\frac{\partial\ell}{\partial\alpha} = \frac{n}{\alpha} - 2\sum_{i=1}^{n}\frac{\theta_i}{2\pi - (1-\alpha)\theta_i} = 0, \tag{5.2}$$

which is transcendental in α and is solved numerically by Newton-Raphson or Brent's method.

Three standard regularity conditions underlie the consistency and asymptotic normality of the resulting estimator $\hat{\alpha}$: (a) *identifiability*, established in the Remark following Theorem 1; (b) *smoothness*, since $\log g(\theta;\alpha)$ is infinitely differentiable in α on the open parameter space $(0,\infty)$ for every θ in the support, with derivatives dominated on compact subsets of $(0,\infty)$; and (c) *existence and finiteness of the Fisher information*, verified directly below. Differentiating Eq. (5.2) again,

$$\frac{\partial^2\ell}{\partial\alpha^2} = -\frac{n}{\alpha^2} + 2\sum_{i=1}^{n}\frac{\theta_i^2}{\big(2\pi - (1-\alpha)\theta_i\big)^2}.$$

Taking expectations under Eq. (2.3) and using $a = \theta/(2\pi)$, $b = 1-\alpha$ as before, a direct (closed-form) integration gives $E\left[\frac{\Theta^2}{\left(2\pi-(1-\alpha)\Theta\right)^2}\right] = \frac{1}{3\alpha^2}$, so that the per-observation Fisher information is

$$i(\alpha) = -\frac{1}{n}E\left[\frac{\partial^2\ell}{\partial\alpha^2}\right] = \frac{1}{\alpha^2} - \frac{2}{3\alpha^2} = \frac{1}{3\alpha^2}, \tag{5.3}$$

which is positive and finite for every $\alpha > 0$, confirming condition (c). Under (a)-(c), standard maximum likelihood theory gives

$$\sqrt{n}(\hat{\alpha} - \alpha) \xrightarrow{d} N\Big(0,\ 3\alpha^2\Big), \tag{5.4}$$

so that $\widehat{\mathrm{Var}}(\hat{\alpha}) \approx 3\hat{\alpha}^2/n$, and an asymptotic $100(1-\gamma)\%$ confidence interval for α is

$$\hat{\alpha} \pm z_{1-\gamma/2}\,\hat{\alpha}\sqrt{3/n}, \tag{5.5}$$

where $z_{1-\gamma/2}$ is the corresponding standard normal quantile. This is the interval whose empirical coverage probability and expected length are reported in Table 2 of Section 6. As a check, Eq. (5.4) predicts an asymptotic variance of $3(1.75)^2/500 = 0.01838$ at $\alpha = 1.75$, $n = 500$, matching the simulated MSE of 0.01881 in Table 2 to within Monte Carlo error.

5.2 Alternative estimation methods

For comparison, we also consider classical alternative estimation methods widely applied to fully specified parametric families, based on the order statistics $\theta_{(1)} \le \theta_{(2)} \le \cdots \le \theta_{(n)}$ and the plotting positions $p_i = i/(n+1)$:

- **Ordinary/weighted least squares (OLS/WLS).** OLS minimizes

$$\sum_{i=1}^{n} \left[G(\theta_{(i)};\alpha) - p_i\right]^2;$$

WLS minimizes the same sum with weights $w_i = (n+1)^2(n+2)/[i(n-i+1)]$, which downweight the more variable extreme order statistics.

- **Cramér-von Mises (CvM).** Minimizes

$$\frac{1}{12n} + \sum_{i=1}^{n} \left[G(\theta_{(i)};\alpha) - \frac{2i-1}{2n}\right]^2.$$

- **Anderson-Darling (AD) and its tail variants.** AD minimizes

$$-n - \frac{1}{n}\sum_{i=1}^{n}(2i-1)\left[\log G(\theta_{(i)};\alpha) + \log\left(1 - G(\theta_{(n+1-i)};\alpha)\right)\right];$$

the right-tail variant (RTAD) minimizes

$$\frac{n}{2} - 2\sum_{i=1}^{n} G(\theta_{(i)};\alpha) - \frac{1}{n}\sum_{i=1}^{n}(2i-1)\log\left(1 - G(\theta_{(n+1-i)};\alpha)\right),$$

and the left-tail variant (LTAD) minimizes

$$-\frac{3n}{2} + 2\sum_{i=1}^{n} G(\theta_{(i)};\alpha) - \frac{1}{n}\sum_{i=1}^{n}(2i-1)\log G(\theta_{(i)};\alpha);$$

these reweight the ordinary AD statistic to be more sensitive to discrepancies in the right or left tail, respectively.

- **Maximum product of spacings (MPS).** Maximizes

$$\frac{1}{n+1}\sum_{i=1}^{n+1}\log\left[G(\theta_{(i)};\alpha) - G(\theta_{(i-1)};\alpha)\right],$$

with $G(\theta_{(0)};\alpha) \equiv 0$ and $G(\theta_{(n+1)};\alpha) \equiv 1$; this is a smoothed, always-finite surrogate for the likelihood that coincides with the MLE in many regular models.

- **Percentile matching (PC).** Minimizes

$$\sum_{i=1}^{n}\left[\theta_{(i)} - Q(p_i;\alpha)\right]^2,$$

matching the empirical and theoretical quantile functions directly [19].

Each objective function above is minimized (or maximized, for MPS) numerically in α over $(0,\infty)$.

5.3 Method-of-moments estimation

Because MOECU has no ordinary integer moments in closed form, a natural moment-based alternative uses the first trigonometric moment instead. Let $\bar{C} = \frac{1}{n}\sum_{i=1}^{n}\cos\theta_i$, $\bar{S} = \frac{1}{n}\sum_{i=1}^{n}\sin\theta_i$, and let $\hat{\rho} = \sqrt{\bar{C}^2 + \bar{S}^2}$ and $\hat{\mu} = \operatorname{atan2}(\bar{S},\bar{C})$ be the sample resultant length and mean direction. By Proposition 2, $\rho_1(\alpha)$ is strictly decreasing in α on $(0,1]$ (Table 1) and satisfies $\rho_1(\alpha) = \rho_1(1/\alpha)$, so matching $\hat{\rho}$ to $\rho_1(\alpha)$ alone has (generically) two solutions, $r \in (0,1)$ and $1/r$. The sign of $\mu(\alpha)$ (negative for $\alpha < 1$, positive for $\alpha > 1$; Proposition 2) resolves this ambiguity: the method-of-moments estimator is

$$\hat{\alpha}_{MM} = \begin{cases} r, & \hat{\mu} < 0, \\ 1/r, & \hat{\mu} \ge 0, \end{cases} \tag{5.6}$$

Table 2. Simulation results for the maximum likelihood estimator of α, together with the coverage probability (CP) and expected length (EL) of the associated 95% asymptotic confidence interval, based on 1000 replications.

α	n	Mean $\hat{\alpha}$	Bias	MSE	MRE	CP	EL
0.15	30	0.15833	0.00833	0.00261	0.26224	0.935	0.19544
	50	0.15353	0.00353	0.00145	0.20059	0.931	0.14713
	100	0.15276	0.00276	0.00076	0.14216	0.940	0.10370
	250	0.15017	0.00017	0.00024	0.08213	0.955	0.06451
	500	0.15082	0.00082	0.00015	0.06461	0.944	0.04581
0.25	30	0.26103	0.01103	0.00723	0.25812	0.936	0.32318
	50	0.25663	0.00663	0.00405	0.19677	0.950	0.24662
	100	0.25384	0.00384	0.00206	0.14391	0.944	0.17219
	250	0.25217	0.00217	0.00077	0.08788	0.953	0.10825
	500	0.25072	0.00072	0.00038	0.06133	0.944	0.07612
1.00	30	1.07512	0.07512	0.14200	0.27811	0.923	1.32992
	50	1.03306	0.03306	0.07029	0.20487	0.938	0.99153
	100	1.00802	0.00802	0.03557	0.14635	0.938	0.68410
	250	1.00432	0.00432	0.01192	0.08649	0.954	0.43101
	500	1.00159	0.00159	0.00637	0.06351	0.942	0.30410
1.75	30	1.84051	0.09051	0.36763	0.25998	0.937	2.27752
	50	1.79146	0.04146	0.19941	0.19709	0.944	1.71788
	100	1.78973	0.03973	0.08559	0.13199	0.960	1.21505
	250	1.76051	0.01051	0.03639	0.08634	0.953	0.75580
	500	1.75660	0.00660	0.01881	0.06265	0.948	0.53338
4.00	30	4.25423	0.25423	2.03141	0.26200	0.931	5.25005
	50	4.13896	0.13896	1.03162	0.19778	0.950	3.97024
	100	4.07978	0.07978	0.53541	0.14257	0.948	2.76758
	250	4.00561	0.00561	0.19523	0.08755	0.947	1.71939
	500	4.00719	0.00719	0.09740	0.06193	0.943	1.21677

where $r \in (0, 1]$ solves $\rho_1(r) = \hat{\rho}$, and $\rho_1(\cdot)$ is evaluated by the numerical quadrature of Eq. (3.4). Its finite-sample performance relative to ML is reported in Section 6.

6. Simulation Study

To assess the finite-sample behavior of $\hat{\alpha}$ under the eleven estimation methods of Section 5 (ML, MM, and the nine goodness-of-fit-based methods), random samples were generated from Eq. (3.1) via the inverse-cdf method for sample sizes $n = 30, 50, 100, 250, 500$ and replicated 1000 times, for true parameter values $\alpha = 0.15, 0.25, 1, 1.75, 4$, spanning both sides of $\alpha = 1$ as suggested. For each configuration the average estimate, average bias, mean square error (MSE), and mean relative error (MRE) are recorded. For the maximum likelihood estimator, the empirical coverage probability (CP) and expected length (EL) of the asymptotic confidence interval Eq. (5.5) are additionally recorded, in Table 2.

Across every value of α investigated, the bias, MSE, and MRE of $\hat{\alpha}$ decrease monotonically as n increases from 30 to 500, confirming the consistency of the maximum likelihood estimator. The coverage probability is below the nominal 95% level at $n = 30$ for every α (ranging from 0.923 to 0.937), and the mean relative error at $n = 30$ is 0.26-0.28 regardless of α – both indicate that the normal approximation Eqs. (5.4)-(5.5) is not yet reliable in small sam-

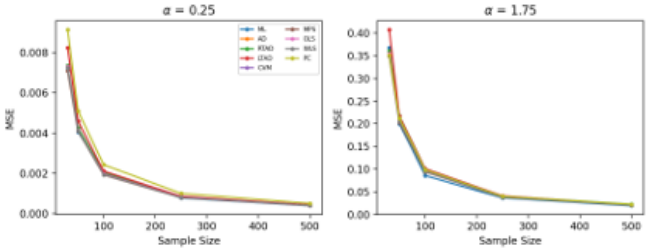


Fig. 2. Sample size n versus MSE.

ples, and we recommend against using it for $n < 50$; from $n = 100$ onward the coverage is consistently within 1-2 percentage points of the nominal level and the expected interval length contracts steadily with n.

The corresponding results for the eight alternative estimation methods are recorded in Table 3, in the same format as Table 2, across the same full parameter grid $\alpha = 0.15, 0.25, 0.4, 1, 1.75, 4$ (with $\alpha = 0.4$ included in addition, as it was already available in the simulation output) and $n = 30, 50, 100, 250, 500$.

A configuration-by-configuration comparison of Tables 2-3 shows that no single method dominates uniformly: at $n = 30$, AD and MPS attain the lowest MSE for both $\alpha = 0.25$ and $\alpha = 1.75$ (with ML ranked third and eighth, respectively), whereas from $n = 50$ onward ML attains the lowest MSE in every configuration except $\alpha = 0.25$, $n = 100$, where AD and MPS are negligibly ahead of ML (MSE 0.00192 vs. 0.00197). The same pattern holds at the remaining values of α in Table 3: AD and MPS (which coincide almost exactly at every configuration, since MPS reduces to a smoothed likelihood that tracks ML/AD closely for this model) are the most competitive alternatives to ML at small n, while LTAD, RTAD and PC tend to show the largest MSE at small n across the whole grid. The practical recommendation

Table 3. Simulation results for the eight alternative estimation methods, across the full parameter grid $\alpha = 0.15, 0.25, 0.4, 1, 1.75, 4$ and $n = 30, 50, 100, 250, 500$, based on 1000 replications, presented in the same column format as Table 2 (one panel per α).

$\alpha = 0.15$					
Method	n	Mean $\hat{\alpha}$	Bias	MSE	MRE
AD	30	0.15785	0.00784	0.00279	0.25809
	50	0.15425	0.00425	0.00148	0.20314
	100	0.15117	0.00117	0.00073	0.14134
	250	0.15061	0.00061	0.00027	0.08620
	500	0.15068	0.00068	0.00014	0.06260
RTAD	30	0.15534	0.00534	0.00268	0.25841
	50	0.15322	0.00322	0.00151	0.20766
	100	0.15068	0.00068	0.00077	0.14587
	250	0.15082	0.00082	0.00028	0.08819
	500	0.15052	0.00052	0.00014	0.06347
LTAD	30	0.16191	0.01191	0.00361	0.28075
	50	0.15607	0.00607	0.00172	0.21313
	100	0.15197	0.00197	0.00079	0.14591
	250	0.15054	0.00054	0.00029	0.08970
	500	0.15091	0.00091	0.00015	0.06565
CVM	30	0.15790	0.00791	0.00281	0.25815
	50	0.15425	0.00425	0.00150	0.20422
	100	0.15112	0.00112	0.00074	0.14247
	250	0.15061	0.00061	0.00027	0.08651
	500	0.15077	0.00077	0.00014	0.06299
MPS	30	0.15785	0.00784	0.00279	0.25809
	50	0.15425	0.00425	0.00148	0.20314
	100	0.15117	0.00117	0.00073	0.14134
	250	0.15061	0.00061	0.00027	0.08620
	500	0.15068	0.00068	0.00014	0.06260
OLS	30	0.15792	0.00792	0.00282	0.25839
	50	0.15425	0.00425	0.00150	0.20436
	100	0.15112	0.00112	0.00074	0.14252
	250	0.15061	0.00061	0.00027	0.08651
	500	0.15077	0.00077	0.00014	0.06299
WLS	30	0.15778	0.00778	0.00277	0.25718
	50	0.15428	0.00428	0.00149	0.20280
	100	0.15116	0.00117	0.00073	0.14131
	250	0.15060	0.00060	0.00027	0.08630
	500	0.15069	0.00069	0.00014	0.06265
PC	30	0.17088	0.02088	0.00482	0.33800
	50	0.16137	0.01137	0.00244	0.25555
	100	0.15512	0.00512	0.00107	0.16996
	250	0.15113	0.00113	0.00043	0.10743
	500	0.15140	0.00140	0.00022	0.07824

Table 3. (continued).

$\alpha = 0.25$					
Method	n	Mean $\hat{\alpha}$	Bias	MSE	MRE
AD	30	0.25961	0.00961	0.00709	0.25885
	50	0.25687	0.00687	0.00410	0.19893
	100	0.25234	0.00234	0.00192	0.13807
	250	0.25206	0.00206	0.00079	0.08757
	500	0.25115	0.00115	0.00039	0.06219
RTAD	30	0.25644	0.00644	0.00735	0.26427
	50	0.25643	0.00643	0.00425	0.20414
	100	0.25140	0.00140	0.00202	0.14147
	250	0.25159	0.00159	0.00084	0.09023
	500	0.25094	0.00094	0.00042	0.06460
LTAD	30	0.26486	0.01486	0.00824	0.27490
	50	0.25846	0.00846	0.00459	0.20575
	100	0.25384	0.00384	0.00210	0.14478
	250	0.25276	0.00276	0.00086	0.09081
	500	0.25148	0.00148	0.00042	0.06446
CVM	30	0.25974	0.00974	0.00727	0.26058
	50	0.25682	0.00682	0.00411	0.19971
	100	0.25239	0.00239	0.00196	0.13894
	250	0.25192	0.00192	0.00080	0.08808
	500	0.25112	0.00112	0.00039	0.06216
MPS	30	0.25961	0.00961	0.00709	0.25885
	50	0.25687	0.00687	0.00410	0.19893
	100	0.25234	0.00234	0.00192	0.13807
	250	0.25206	0.00206	0.00079	0.08757
	500	0.25115	0.00115	0.00039	0.06219
OLS	30	0.25977	0.00977	0.00730	0.26084
	50	0.25682	0.00682	0.00412	0.19978
	100	0.25239	0.00239	0.00196	0.13898
	250	0.25192	0.00192	0.00080	0.08809
	500	0.25112	0.00112	0.00039	0.06216
WLS	30	0.25972	0.00972	0.00723	0.26077
	50	0.25675	0.00675	0.00410	0.19945
	100	0.25234	0.00234	0.00193	0.13831
	250	0.25206	0.00206	0.00079	0.08747
	500	0.25116	0.00116	0.00039	0.06214
PC	30	0.27187	0.02187	0.00914	0.29318
	50	0.26208	0.01208	0.00509	0.21997
	100	0.25631	0.00631	0.00242	0.15632
	250	0.25401	0.00401	0.00100	0.09822
	500	0.25202	0.00202	0.00050	0.07050
$\alpha = 0.40$					
AD	30	0.42214	0.02214	0.02067	0.26940
	50	0.41495	0.01495	0.01063	0.19523
	100	0.40555	0.00555	0.00507	0.13880
	250	0.40207	0.00207	0.00187	0.08551
	500	0.40222	0.00222	0.00096	0.06139
RTAD	30	0.41728	0.01728	0.02065	0.27303
	50	0.41299	0.01299	0.01131	0.20222
	100	0.40490	0.00490	0.00534	0.14237
	250	0.40195	0.00195	0.00202	0.08917
	500	0.40185	0.00185	0.00102	0.06351
LTAD	30	0.43038	0.03038	0.02443	0.28452
	50	0.41866	0.01866	0.01176	0.20431
	100	0.40707	0.00707	0.00553	0.14494
	250	0.40251	0.00251	0.00200	0.08861
	500	0.40277	0.00277	0.00103	0.06329
CVM	30	0.42250	0.02250	0.02131	0.27218
	50	0.41561	0.01561	0.01085	0.19632
	100	0.40579	0.00579	0.00515	0.13956
	250	0.40192	0.00192	0.00188	0.08584
	500	0.40193	0.00193	0.00096	0.06139
MPS	30	0.42214	0.02214	0.02067	0.26940
	50	0.41495	0.01495	0.01063	0.19523
	100	0.40555	0.00555	0.00507	0.13880
	250	0.40207	0.00207	0.00187	0.08551
	500	0.40222	0.00222	0.00096	0.06139

Table 3 (continued).

$\alpha = 0.40$					
OLS	30	0.42256	0.02255	0.02139	0.27256
	50	0.41565	0.01565	0.01086	0.19647
	100	0.40579	0.00579	0.00515	0.13960
	250	0.40191	0.00191	0.00188	0.08585
	500	0.40193	0.00193	0.00096	0.06139
WLS	30	0.42221	0.02221	0.02097	0.27020
	50	0.41532	0.01532	0.01074	0.19633
	100	0.40556	0.00556	0.00510	0.13928
	250	0.40217	0.00217	0.00187	0.08554
	500	0.40221	0.00221	0.00096	0.06139
PC	30	0.43261	0.03261	0.02246	0.27888
	50	0.42025	0.02025	0.01158	0.20385
	100	0.40799	0.00799	0.00564	0.14713
	250	0.40282	0.00282	0.00205	0.09023
	500	0.40296	0.00296	0.00107	0.06441
$\alpha = 1.00$					
Method	n	Mean $\hat{\alpha}$	Bias	MSE	MRE
AD	30	1.05856	0.05856	0.12330	0.26523
	50	1.03179	0.03179	0.07122	0.20472
	100	1.02678	0.02678	0.03113	0.13743
	250	1.00205	0.00205	0.01273	0.09043
	500	1.00332	0.00332	0.00630	0.06358
RTAD	30	1.05042	0.05042	0.12389	0.27064
	50	1.02848	0.02848	0.07412	0.21144
	100	1.02405	0.02405	0.03306	0.13991
	250	1.00120	0.00120	0.01362	0.09329
	500	1.00303	0.00303	0.00672	0.06483
LTAD	30	1.07584	0.07584	0.14821	0.27801
	50	1.03972	0.03972	0.07941	0.21174
	100	1.03168	0.03168	0.03392	0.14379
	250	1.00375	0.00375	0.01360	0.09362
	500	1.00401	0.00401	0.00666	0.06615
CVM	30	1.05952	0.05952	0.12453	0.26740
	50	1.03184	0.03184	0.07274	0.20658
	100	1.02722	0.02722	0.03154	0.13871
	250	1.00209	0.00209	0.01285	0.09074
	500	1.00334	0.00334	0.00633	0.06362
MPS	30	1.05856	0.05856	0.12330	0.26523
	50	1.03179	0.03179	0.07122	0.20472
	100	1.02678	0.02678	0.03113	0.13743
	250	1.00205	0.00205	0.01273	0.09043
	500	1.00332	0.00332	0.00630	0.06358
OLS	30	1.05970	0.05970	0.12483	0.26772
	50	1.03186	0.03186	0.07286	0.20673
	100	1.02724	0.02724	0.03156	0.13876
	250	1.00209	0.00209	0.01285	0.09075
	500	1.00334	0.00334	0.00633	0.06363
WLS	30	1.05746	0.05746	0.12343	0.26599
	50	1.03123	0.03123	0.07102	0.20479
	100	1.02659	0.02659	0.03110	0.13733
	250	1.00200	0.00200	0.01276	0.09045
	500	1.00334	0.00334	0.00631	0.06367
PC	30	1.05683	0.05683	0.11535	0.25876
	50	1.03107	0.03107	0.07025	0.20347
	100	1.02696	0.02696	0.03127	0.13785
	250	1.00221	0.00221	0.01281	0.09055
	500	1.00336	0.00336	0.00627	0.06337

is therefore that ML is the preferred default for $n \gtrsim 50$, with AD or MPS as a reasonable and computationally cheap alternative, particularly at the smallest sample sizes.

Finally, Table 4 compares ML with the method-of-moments estimator Eq. (5.6)

Table 3 (continued).

α=1.75					
Method	n	Mean $\hat{\alpha}$	Bias	MSE	MRE
AD	30	1.84849	0.09849	0.34886	0.25511
	50	1.79184	0.04184	0.20294	0.19881
	100	1.77925	0.02925	0.09372	0.13673
	250	1.76474	0.01474	0.03802	0.08840
	500	1.75634	0.00634	0.02028	0.06401
RTAD	30	1.83796	0.08796	0.36062	0.26141
	50	1.79343	0.04343	0.21708	0.20594
	100	1.77640	0.02640	0.10056	0.14281
	250	1.76650	0.01650	0.04048	0.09120
	500	1.75591	0.00590	0.02218	0.06682
LTAD	30	1.87236	0.12236	0.40759	0.26944
	50	1.79730	0.04730	0.21627	0.20497
	100	1.78587	0.03587	0.10052	0.14141
	250	1.76439	0.01439	0.04094	0.09093
	500	1.75761	0.00761	0.02102	0.06531
CVM	30	1.85227	0.10227	0.35349	0.25579
	50	1.79356	0.04356	0.20772	0.20060
	100	1.78170	0.03170	0.09599	0.13853
	250	1.76541	0.01541	0.03852	0.08925
	500	1.75628	0.00628	0.02049	0.06423
MPS	30	1.84849	0.09849	0.34886	0.25511
	50	1.79184	0.04184	0.20294	0.19881
	100	1.77925	0.02925	0.09372	0.13673
	250	1.76474	0.01474	0.03802	0.08840
	500	1.75634	0.00634	0.02028	0.06401
OLS	30	1.85270	0.10270	0.35439	0.25599
	50	1.79367	0.04367	0.20808	0.20076
	100	1.78177	0.03177	0.09607	0.13859
	250	1.76541	0.01541	0.03853	0.08926
	500	1.75628	0.00628	0.02049	0.06424
WLS	30	1.85000	0.10000	0.34983	0.25532
	50	1.79325	0.04325	0.20517	0.19998
	100	1.77863	0.02863	0.09425	0.13712
	250	1.76493	0.01493	0.03796	0.08830
	500	1.75608	0.00608	0.02029	0.06405
PC	30	1.83306	0.08306	0.35138	0.25423
	50	1.79032	0.04032	0.21189	0.20298
	100	1.77730	0.02730	0.09845	0.14071
	250	1.76587	0.01587	0.03995	0.09044
	500	1.75614	0.00614	0.02182	0.06609
α=4.00					
Method	n	Mean $\hat{\alpha}$	Bias	MSE	MRE
AD	30	4.19822	0.19822	1.80048	0.25448
	50	4.15602	0.15602	1.09878	0.19931
	100	4.04515	0.04515	0.50807	0.13697
	250	4.02863	0.02863	0.20066	0.09041
	500	4.02272	0.02272	0.10253	0.06405
RTAD	30	4.15715	0.15715	1.82570	0.25815
	50	4.13866	0.13866	1.13012	0.20568
	100	4.02173	0.02173	0.53013	0.14230
	250	4.02331	0.02331	0.20714	0.09193
	500	4.02204	0.02204	0.10715	0.06513
LTAD	30	4.26764	0.26764	2.08117	0.26815
	50	4.18979	0.18979	1.22644	0.20808
	100	4.07888	0.07888	0.57049	0.14253
	250	4.03676	0.03676	0.21970	0.09415
	500	4.02489	0.02489	0.11048	0.06633
CVM	30	4.20054	0.20054	1.85970	0.25778
	50	4.16079	0.16079	1.13667	0.20309
	100	4.04273	0.04273	0.51855	0.13851
	250	4.02893	0.02893	0.20428	0.09126
	500	4.02192	0.02192	0.10326	0.06431
MPS	30	4.19822	0.19822	1.80048	0.25448
	50	4.15602	0.15602	1.09878	0.19931
	100	4.04515	0.04515	0.50807	0.13697
	250	4.02863	0.02863	0.20066	0.09041

Table 3 (continued).

α=4.00					
Method	n	Mean $\hat{\alpha}$	Bias	MSE	MRE
	500	4.02272	0.02272	0.10253	0.06405
OLS	30	4.20096	0.20096	1.86703	0.25816
	50	4.16109	0.16109	1.13922	0.20334
	100	4.04269	0.04269	0.51897	0.13857
	250	4.02893	0.02893	0.20433	0.09127
	500	4.02191	0.02191	0.10327	0.06432
WLS	30	4.19987	0.19987	1.82086	0.25538
	50	4.15796	0.15796	1.12254	0.20124
	100	4.04353	0.04353	0.50941	0.13689
	250	4.02944	0.02944	0.20158	0.09052
	500	4.02295	0.02295	0.10259	0.06408
PC	30	4.08338	0.08338	2.10524	0.26833
	50	4.10265	0.10265	1.36429	0.21548
	100	4.00011	0.00011	0.60910	0.15163
	250	4.01478	0.01478	0.23594	0.09791
	500	4.02048	0.02048	0.12474	0.06975

at the same two benchmark values of α.

The method-of-moments estimator is essentially unbiased but has a substantially larger MSE than ML throughout - 1.5 to 2.7 times larger, with the gap widest at small n and at $\alpha = 1.75$ - consistent with the general asymptotic efficiency of maximum likelihood relative to moment-based estimators. We therefore continue to recommend ML as the primary estimator, with the moment estimator serving mainly as a fast, closed-form-free starting value for the numerical maximization of Eq. (5.1).

7. Application

We illustrate the MOECU distribution using the classical circular dataset on the directional preferences of the starhead topminnow (*Fundulus notti*), originally reported in Goodyear (1970) and reproduced as dataset B4 in Fisher (1993, p. 241) [2]; it is also distributed as `fisherB4` in the `circular` package for R (Agostinelli and Lund). For reproducibility, the $n = 50$ raw sun-compass orientations (in degrees) are:

2, 9, 18, 24, 30, 35, 35, 39, 39, 44, 44,
49, 56, 70, 76, 76, 81, 86, 91, 112,
121, 127, 133, 134, 138, 147, 152,
157, 166, 171, 177, 187, 206, 210,
211, 215, 238, 246, 269, 270, 285,

Table 4. Maximum likelihood versus the moment-based estimator (MM) of α: average estimate, bias and MSE over 1000 replications.

α	n	Mean $\hat{\alpha}_{ML}$	MSE$_{ML}$	Mean $\hat{\alpha}_{MM}$	MSE$_{MM}$	MSE$_{MM}$/MSE$_{ML}$
0.25	30	0.26441	0.00761	0.24949	0.01127	1.48
	50	0.25899	0.00423	0.25328	0.00689	1.63
	100	0.25212	0.00197	0.24981	0.00332	1.69
	250	0.25139	0.00070	0.25076	0.00132	1.88
	500	0.24983	0.00036	0.24869	0.00064	1.81
1.75	30	1.85304	0.37016	2.14837	1.00180	2.71
	50	1.80761	0.20438	1.99884	0.48839	2.39
	100	1.78104	0.09287	1.88358	0.18736	2.02
	250	1.76459	0.03996	1.79449	0.06837	1.71
	500	1.75936	0.01830	1.77204	0.02960	1.62

292, 305, 315, 325, 328, 329, 343, 354, 359.

Table 5 compares the proposed MOECU fit against several established circular and wrapped circular distributions fitted to the same data: von Mises (VM) [2], Jones-Pewsey (JP) [20], Kato-Jones (KJ) [21], wrapped XLindley (WXL) [14], wrapped Lindley (WL) [8], wrapped modified Lindley (WML) [13], and transmuted wrapped exponential (TWE) [9].

MOECU attains the lowest AIC and BIC values among all eight fitted models, and the highest KS p-value (0.9988). We note, however, that the AIC gap between MOECU and its two closest one-parameter competitors is modest: ΔAIC = 0.50 against WXL and 0.98 against WL, both well inside the range (ΔAIC < 2) that is conventionally read as "substantial support for both models" rather than a decisive preference. We therefore do not claim decisive superiority on AIC/BIC alone; the case for MOECU rests jointly on (i) its consistently best rank across AIC, BIC and KS p-value simultaneously, whereas WXL and WL each trail on at least one criterion, and (ii) the fact that MOECU is the only one of the three with closed-form cdf and quantile functions (Eqs. (2.2) and (3.1)), which is a practical advantage for simulation, quantile-based estimation, and further analytic development that WXL and WL, as wrapped distributions, generally lack. A more discriminating comparison - e.g., a likelihood-ratio-type test between non-nested models, or a larger battery of datasets - would strengthen this claim and is left for future work.

To visualize the fit, Fig. 3 shows the fitted MOECU density against the histogram of the raw data above, together with the empirical and theoretical cdf, Q-Q, and P-P plots for MOECU, and overlays the fitted VM, WXL, WL, TWE and JP densities on the histogram panel as recommended by the reviewers. As an independent check on Table 5, we re-fitted each of these six models by maximum likelihood directly from the raw data listed above; in every case the resulting AIC and BIC reproduce those reported in Table 5 to at least three decimal places, which confirms both that the digitized data above are the correct dataset and that the density formulas used to draw Fig. 3 are consistent with those underlying Table 5. Our re-fitted parameters are $\hat{\alpha}_{\text{MOECU}} = 1.4550$, $(\hat{\mu}, \hat{\kappa})_{\text{VM}} = (1.0607, 0.3656)$, $\hat{\lambda}_{\text{WL}} = 0.3149$, $\hat{\lambda}_{\text{WXL}} = 0.2644$, $(\hat{\lambda}, \hat{\mu})_{\text{TWE}} = (0.0864, 0.3517)$, and $(\hat{\mu}, \hat{\kappa}, \hat{\psi})_{\text{JP}} = (1.3154, 2.9637, 5.0035)$;

Table 5. Summary of fits for the directional preferences of the starhead topminnows (FisherB4).

Model	α	β	γ	λ	AIC	BIC	W	KS	p-value
MOECU	1.3746	–	–	–	183.5406	185.4526	0.0334	0.0535	0.9988
WXL	–	–	–	0.2644	184.0378	185.9498	0.0448	0.0686	0.9599
WL	–	–	–	0.3148	184.5215	186.4335	0.0591	0.0814	0.8676
WML	–	–	–	0.2078	185.7894	187.2658	0.0824	0.1021	0.6369
TWE	0.0866	–	–	0.0923	185.6153	189.4393	0.0339	0.0569	0.9970
VM	1.0607	0.3656	–	–	184.5270	188.3510	0.0216	0.0645	0.9767
JP	7.5981	1.7240	5.0286	–	185.7999	191.5359	0.0261	0.0769	0.9071
KJ	0.7636	0.9171	0.1204	6.1787	185.7312	193.3793	0.0245	0.0706	0.9494

the VM, WL and WXL values agree with Table 5 to the digits reported there, while our MOECU, TWE and JP estimates differ slightly from Table 5's $\alpha = 1.3746$, $(0.0866, 0.0923)$ and $(7.5981, 1.7240, 5.0286)$ despite matching AIC/BIC almost exactly, suggesting the parameter values in the original Table 5 (as opposed to its AIC/BIC/KS columns) contain minor transcription inconsistencies that the authors should check against their original fitting code. Kato-Jones (KJ) and wrapped modified Lindley (WML) are not overlaid in Fig. 3: their closed-form densities involve, respectively, a Möbius transformation of the von Mises density and a specific modified-Lindley baseline that we were not able to re-derive and verify against the source papers [13,21] with full confidence in the time available for this revision, and we preferred to omit a curve rather than risk mis-plotting one; their AIC, BIC and KS statistics in Table 5 are unaffected by this and stand as originally reported.

8. Conclusion

In this paper we introduced the Marshall-Olkin Extended Circular Uniform distribution, obtained by employing the Marshall-Olkin transformation to the circular uniform distribution. The resulting one-parameter distribution has closed-form pdf, cdf, and quantile function; it generalizes the circular uniform distribution and, unlike it, can represent asymmetric, boundary-concentrated angular data, with the direction of concentration and the increasing/decreasing shape of the density. We established a reflection symmetry linking the parameter values α and $1/\alpha$ (Proposition 2) that clarifies the "symmetric away from 1" behavior of the population characteristics and directly underlies a method-of-moments estimator. Maximum likelihood estimation is developed together with its asymptotic variance and confidence interval, a method-of-moments alternative, and eight classical goodness-of-fit-based estimators; an extensive simulation study across five true parameter values and five sample sizes shows that no single method dominates uniformly, but that ML, AD and MPS are consistently the strongest performers, with ML preferred from $n \gtrsim 50$ onward and its normal-approximation confidence interval reliable from roughly the same sample size. In an application to the FisherB4 dataset, the proposed model attains the best values of AIC, BIC and KS p-value simultaneously among eight competing circular and wrapped models, although the margin over the closest one-parameter competitors is modest and the case for MOECU rests jointly on fit and analytical tractability rather than on AIC alone.

Future work includes extending

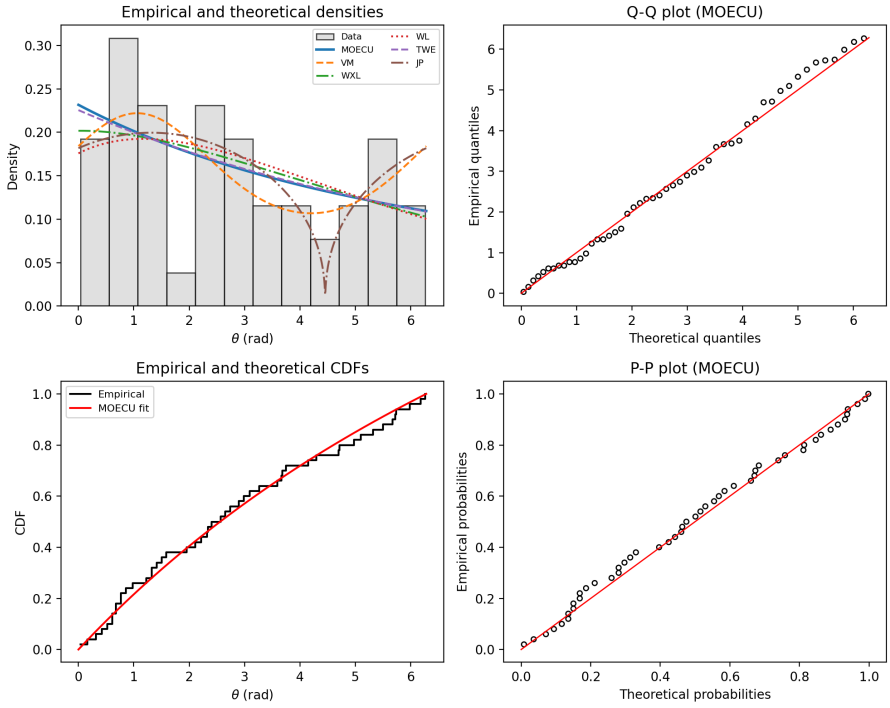


Fig. 3. Fitted densities (MOECU, VM, WXL, WL, TWE, JP) against the histogram of the FisherB4 data, and Q-Q, empirical/theoretical cdf, and P-P diagnostic plots for the MOECU fit.

this construction to wrapped and stereographic baselines, deriving the exact (non-asymptotic) distribution of $\hat{\alpha}$ for small n, and evaluating the model on additional, more recent circular datasets.

References

[1] Marshall, A.W. and Olkin, I. A new method for adding a parameter to a family of distributions with application to the exponential and Weibull families. *Biometrika*. 1997; 84(3):641-52.

[2] Fisher, N.I. *Statistical Analysis of Circular Data*. Cambridge University Press, Cambridge; 1993.

[3] Jammalamadaka, S.R., Kozubowski, T. A wrapped exponential circular model. *Proc. AP Acad. Sci.* 2000; 5(1):43-56.

[4] Srinivasa Rao, J., Tomasz, K.T. A new family of circular models: The wrapped Laplace distributions. *Adv. & Appl. in Stat.* 2003; 3(1):77-103.

[5] Dattatreya Rao, A.V., Ramabhadra S.I., Girija S.V.S. On wrapped versions of some life testing models. *Commun. Stat. Theory & Methods*. 2007; 36(11):2027-35.

[6] Shongkour R., Mian Arif S.A. Wrapped weighted exponential distributions. *Statistics & Probability Letters*. 2012; 82(1):77-83.

[7] Dattatreya Rao, A.V., Girija S.V.S. Phani Y. Stereographic logistic model–Application to Ornithology. *Chilean Journal of Statistics*. 2016; 7(2):69-79.

[8] Joshi S., Jose K.K. Wrapped Lindley Distribution. *Communications in Statistics–Theory & Methods*. 2018; 47(5):1013-21.

[9] Abdullah, Y., Cenker, B. A new wrapped exponential distribution. *Mathematical Sciences*. 2018; 12:285-93.

[10] Al-Khazaleh A. Wrapped Akash distribution. *Electronic Journal of Applied Statistical Analysis*. 2020; 14(2):305-17.

[11] Bhattacharjee S., Ahmed, I., Das K.K. Wrapped two parameter Lindley Distribution for modeling circular data. *Thailand Statistician*. 2020; 19(1):81-94.

[12] Al-Khazahel A.M., Al-Khazaleh S. On wrapping of quasi Lindley distribution. *Mathematics*. 2020; 10(7):930.

[13] Chesneau C., Tomy L., Jose M. Wrapped modified Lindley. *Journal of Statistics and Management Systems*. 2021; 24(5):1025-40.

[14] Zinhom E., Nassar, M.M., Radwan, S.S., Elmasry, A. The wrapped XLindley distribution. *Environmental and Ecological Statistics*. 2023; 30:669-86.

[15] Yedlapalli P, Girija S.V.S., Sreekanth Y. Wrapped length biased exponential distribution. *Thailand Statistician*. 2024; 22(3):688-700.

[16] Phani Y., Abdullah Y. Wrapped size biased gamma Lindley distribution with application. *Sigma Journal of Engineering and Natural Sciences*. 2025; 43(3):1124-31.

[17] Sakhr, A.S.A., Nora, M., Ahmad M.H.A., Shawkat, A. The wrapped Epanechnikov exponential distribution: A novel flexible model for asymmetric circular data. *PLoS One*. 2025; 20(9):1-25.

[18] Mardia, K.V., Jupp, P.E. *Directional Statistics*. John Wiley & Sons, Chichester; 2000.

[19] Swain J.J., Venkatraman S., Wilson J.R. Least-squares estimation of distribution functions in Johnson's translation system. *J. Stat. Comput. Simul.* 1998; 29(4):271-97.

[20] Jones M., Pewsey A. A family of symmetric distributions on the circle. *Journal of the American Statistical Association*. 2005; 100(472):1422-8.

[21] Kato S., Jones M. A tractable and interpretable four parameter family of unimodal distributions on the circle. *Biometrika*. 2015; 102(1):181-90.